ЯДЕРНА ФІЗИКА
NUCLEAR PHYSICS

УДК 539.142 https://doi.org/10.15407/jnpae2024.02.105

N. P. Saeed Abdulla[1], A. Pavithran[1], M. K. Preethi Rajan[2], R. K. Biju[1,3,*]

[1] *Department of Physics, Government Brennen College, Dharmadam, Thalassery, Kerala, India*
[2] *Department of Physics, Payyanur College, Kannur University, Payyanur, Kannur, Kerala, India*
[3] *Department of Physics, Pazhassi Raja N. S. S. College, Mattanur, Kannur University, Kannur, Kerala, India*

*Corresponding author: bijurkn@gmail.com

INVESTIGATION OF TWO-PROTON DECAY USING MODIFIED FORMATION PROBABILITY

In this study, we investigated two-proton radioactivity using the two-potential approach with a cosh-type potential to calculate the half-lives. The depth parameter V_0 = 58.405 MeV and diffuseness a = 0.537 fm in the cosh-type nuclear potential show the lowest standard deviation between the calculated and experimental half-lives. We proposed a linear formula for the formation probability using the linear relationship between $\log_{10}S_{2p}$ and $A_d^{1/3}$ for the angular momentum state l = 0, 2 and 4. The model achieved the lowest standard deviation (σ = 1.09) using this linear formula compared to previous models and empirical formulas. The proposed formula significantly improved the accuracy of half-life predictions by reducing the standard deviation from 1.73 to 1.09. The predicted half-lives exhibit a hindrance factor in the range of −1.62 to 2.42, which is the lowest compared to earlier theoretical predictions. These results indicate that the proposed linear formation probability formula is suitable for reproducing experimental half-lives. The linear formula for formation probability was generalized for different angular momentum states by conducting least squares fit. We extended the half-life and formation probability predictions to 48 nuclei, and the predicted half-lives are in good agreement with the previous five theoretical models and two empirical formula predictions.

Keywords: two-potential approach, formation probability.

1. Introduction

In two-proton radioactivity, two protons are simultaneously emitted from nuclei near the proton drip line. This exotic and rare radioactive decay process was first predicted by the theoretical physicist Zeldovich in 1960 [1]. This phenomenon involves a quantum tunneling process wherein two-protons tunnel through the potential barrier of the parent nucleus. Studies on two-proton radioactivity provide valuable information about the nucleus' structure, stability, and nucleon interactions. The experimental detection of two-proton decay is challenging due to its rarity. Currently, several theoretical studies on two-proton radioactivity are ongoing, utilizing different theoretical models and approaches, which will be helpful for future experimental investigations.

Goldanskii [2, 3] and Jänecke [4] initiated theoretical investigations into nuclei to find the nuclei that emit protons, while Galitsky and Cheltsov [5] provided the first theoretical description of two-proton emission. Currently, numerous theoretical models and empirical formulas have successfully explained both one-proton and two-proton radioactivity utilising various models such as the screened electrostatic barrier (SEB) [6], the Gamow-like model (GLM) [7], the diproton model [8], the three-body model [9], the simultaneous and sequential decay model [10], the Coulomb and proximity potential model (CPPM) [11], and the unified fission model (UFM) [12] to study two-proton radioactivity. Srinivas et al [13, 14] conducted a comprehensive study on proton emission, including the proton emission half-lives of different lanthanide isotopes using different proximity functions, the investigation into almost all super heavy nuclei with atomic number Z = 104 - 126, and the study of proton decay in almost all actinide nuclei [15, 16]. The authors [17] also systematically studied proton radioactivity half-lives in the atomic number range $53 \leq Z \leq 83$ using macroscopic models such as the CPPM, effective liquid drop model (ELDM), generalized liquid drop model (GLDM), universal decay law for proton emission (UDLP), GLM, and UFM. Recently, the authors [18] proposed semi-empirical formulas to predict one-proton and two-proton decay half-lives, also explaining radioactivity using well-accepted models such as the CPPM, ELDM, GLDM, and modified GLDM. Manjunatha et al. studied proton radioactivity of heavy nuclei in the atomic number range $72 < Z < 88$ [19] and also investigated super heavy nuclei with magic numbers of neutrons and protons [20]. Saeed Abdulla et al. investigated two-proton radioactivity using the ELDM with VMAS-EFF combinations [21] and proposed empirical formulas to compute the half-life of both one-proton and two-proton radioactivity [22, 23].

Pan et al. [24] utilized the Skyrme - Hartree - Fock method to study two-proton decay, and Brown et al. [25] applied the R-matrix method to compute the half-life of two-proton decay in the nucleus ^{45}Fe. Rotureau et al. [26] used the continuous shell model to explain two-proton emission in nuclei like ^{45}Fe, ^{48}Ni, and ^{54}Zn, while Cui et al. [27] employed the GLDM to estimate the half-lives of ground-state nuclei. Goncalves et al. [28] utilized the ELDM to determine the half-lives of two-proton emissions for atomic masses below 70. Furthermore, several empirical formulas have been suggested for accurately estimating the half-life of two-proton decay. Sreeja et al. [29] introduced a four-parameter empirical formula for two-proton decay half-lives, and Liu et al. [30] proposed a new Geiger-Nuttall law for estimating the half-lives of two-proton decays.

The confirmation of two-proton radioactivity has been delayed due to limitations in detection technologies and radioactive beam facilities. After a few decades, KeKelis et al. [31] successfully confirmed the two-proton emission widths of ^{12}O and ^{16}Ne. Kryger et al. [32] utilized a ^{13}O projectile via single neutron stripping to detect two-proton emission in ^{12}O. In 2002, two-proton decay was experimentally confirmed in the ground state of the ^{45}Fe isotope at GSI [33] and GANIL [34]. The two-proton emission in the ^{54}Zn nucleus was identified experimentally at GANIL [35] in 2005. Later, the two-proton decay of ^{48}Ni was also discovered [36]. In 2007, Mukha et al. [37] identified two-proton radioactivity in ^{19}Mg by analyzing the resulting decay products. Further experiments with the BigRIPS separator confirmed the detection of two-proton emissions from ^{67}Kr [38]. Extremely short-lived two-proton emission has been experimentally observed in ^{6}Be [39] and ^{16}Ne [40] nuclei.

Buck et al. [41, 42] proposed a cluster model approach using a parameterized cosh-type nuclear potential to investigate decay phenomena. Several theoretical studies have been conducted on alpha decay using a TPA and cosh-type potential. Deng et al. studied the nucleus ^{296}Og [43], while Sun et al. investigated the half-lives of doubly odd nuclei [44]. Chen et al. [45] used the TPA and a cosh-type potential to study one-proton decay. Zhang et al. [46] also investigated proton decay using the improved cluster model with a cosh-type nuclear potential. Formation probability or spectroscopic factor is important in estimating the decay half-life. There are several methods to study the formation probability, such as various semi-microscopic techniques, including the implementation of relativistic continuum Hartree - Bogoliubov [47], the application of relativistic mean field theory with the BCS method [48], and the covariant density functional with the BCS method [49]. Moreover, there are phenomenological methods available to investigate the formation probability. Chen et al. [45] have recently proposed a linear relationship that connects the formation probability of one-proton decay process with the cube root of the atomic mass of the daughter nucleus. We studied the two-proton decay using the TPA and the cosh-type nuclear potential in the present work. Also, we investigated the relationship between formation probability and the cube root of the atomic mass of the daughter nucleus to find a new formula for formation probability.

2. The model

The total interaction potential in the TPA is the sum of the Coulomb potential, centrifugal potential, and nuclear potential. Which can be expressed as

$$V(r) = V_C(r) + V_l(r) + V_N(r). \quad (1)$$

The Coulomb potential is calculated by considering the nucleus as a uniformly charged sphere, and it can be expressed as

$$V_C(r) = \frac{Z_{2p}Z_d e^2}{2R}\left[3 - \frac{r^2}{R^2}\right] \quad \text{for } r \le R, \quad (2)$$

$$\frac{Z_{2p}Z_d e^2}{2r} \quad \text{for } r > R. \quad (3)$$

The atomic numbers Z_{2P} and Z_d correspond to the 2p fragment nucleus and daughter nucleus, respectively, and A is the mass number of the parent nucleus. The sharp radius R is calculated using the formula $R = r_0 A^{1/3}$. In the current work, r_0 is taken as 1.2 fm [50]. The Langer-modified centrifugal barrier [51] is utilized for calculating the centrifugal potential, and it is calculated as

$$V_{l(r)} = \frac{\hbar^2 (l + \frac{1}{2})^2}{2\,\mu\, r^2}, \quad (4)$$

where μ and l denote the reduced mass of the decaying nuclear system and the orbital angular momentum, respectively. By applying the conservation laws of parity and angular momentum, we determined the orbital angular momentum (l) of the two-proton fragments. The cosh-parameterized nuclear potential proposed by Buck et al. [52] is used to compute nuclear potential and it can be expressed as

$$V_N(r) = -\lambda V_0 \frac{1 + \cosh(R/a)}{\cosh(r/a) + \cosh(R/a)}, \quad (5)$$

where λ, V_0, a, and R are the renormalization factor,

depth of nuclear potential, diffuseness parameters, and sharp radius, respectively. For each case of decay, the Bohr - Sommerfeld quantization condition is used to find the renormalization factor [53].

$$\int_{r_1}^{r_2}\sqrt{\frac{2\mu}{\hbar^2}\left[Q_{2P}-V(r)\right]}dr=(G-l+1)\frac{\pi}{2}. \quad (6)$$

In the current calculation for two-proton decay, where $G = 2n + l$ represents the principal quantum number, values of $G = 4$ or 5 are chosen for $l = 0$, 2, and 4. Γ_{2p} is the width of two-proton decay which can be obtained by WKB method

$$\Gamma_{2p}=S_{2p}\frac{\hbar^2 FP}{4\mu}, \quad (7)$$

where S_{2p} is the formation probability of two-proton radioactivity. The normalized factor (F) can be calculated as

$$F\int_{r_1}^{r_2}\frac{1}{2k(r)}dr=1. \quad (8)$$

The penetration probability (P) is calculated using the WKB approximation.

$$P=\exp\left\{-2\int_{r_2}^{r_3}k(r)dr\right\}. \quad (9)$$

The distance between the centers of two protons and the daughter nucleus is represented as r. The classical turning points r_1, r_2 and r_3 are calculated using the conditions $V(r) = Q_{2p}$. The wave number of the emitted two protons can be calculated as

$$k(r)=\sqrt{\frac{2\mu}{\hbar^2}\left[Q-V(r)\right]}. \quad (10)$$

The decay energy is computed using the mass excess taken from the Mass table by Wang et al. [54]. The decay energy is calculated as

$$Q=\Delta M_{(A,Z)}-\left(\Delta M_{(A-2,Z-2)}+\Delta M_{2p}\right). \quad (11)$$

ΔM_{2p}, $\Delta M_{(A\text{-}2,Z\text{-}2)}$, and $\Delta M_{(A,Z)}$ are the two protons, daughter and parent, nuclei's mass excess, respectively. The half-life of two-proton radioactivity is calculated by the following equation

$$T_{1/2}=\frac{\hbar \ln 2}{\Gamma_{2p}}. \quad (12)$$

3. Result and discussions

In the present study, we investigated two-proton radioactivity utilizing the TPA and a cosh-type nuclear potential. In the TPA, the total interaction potential is the sum of the Coulomb, centrifugal, and nuclear potentials. We plotted a graph to illustrate the behaviour of each variation potential with the separation radius r for the nucleus ^{54}Zn in Fig. 1.

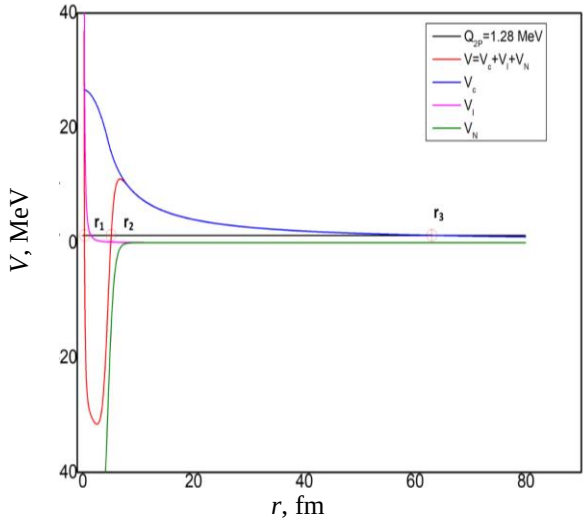

Fig. 1. Variation of Coulomb, centrifugal, nuclear and total interaction potentials with separation radius r for nucleus ^{54}Zn. (See color Figure on the journal website.)

From the Figure, it is clear that the total potential coincided with the experimentally observed Q_{2P} value of 1.28 MeV [55], which corresponds to the classical turning points. In Fig. 1, we found three classical turning points that satisfy the condition $V(r) = Q_{2P}$. We used the depth parameter $V_0 = 58.405$ MeV and diffuseness ($a = 0.537$ fm) to calculate the cosh-type nuclear potential, which exhibited the lowest standard deviation between the calculated and experimental half-lives. To check the accuracy of the model's predictions, we computed the half-lives of experimentally observed decay cases using the TPA and cosh-type nuclear potential. The formation probability plays an essential role in estimating the two-proton decay half-life. The formation probability is also called the spectroscopic factor because it relates to various nuclear structure properties. One method to measure the experimental formation probability (S_{2P}) is to compare the estimated two-proton radioactivity half-life to the observed experimental half-life. The experimental formation probability of two-proton decay is calculated as

$$S_{2P}^{exp}=S_0 T_{1/2}^{cal}/T_{1/2}^{exp}. \quad (13)$$

We use the approximation $S_0 = 0.5$ [56] to compute the half-life of two-proton decay and use Eq. (13) to find the corresponding experimental formation probability. The resulting logarithmic half-life values and experimental formation probability values are presented in the fourth and fifth columns of Table 1. We have included the experimentally measured half-lives and decay energies of two-proton radioactivity in the second and third columns for comparison.

Table 1. **Comparison of calculated logarithmic half-lives for two-proton decay isotopes with experimental half-lives**

Nucleus	Q_{2p}^{Exp}, MeV	$\log_{10} T_{1/2}^{Exp}$, s	$\log S_{2P}^{Exp}$	$\log_{10}T_{1/2}$, s	$\log_{10}T_{1/2}$, s
^{6}Be	1.371(5) [38]	–19.51 [38]	–1.677	–20.886	–21.127
^{12}O	1.638(24) [57]	–19.4 [57]	–0.919	–20.018	–19.724
	1.820(120) [31]	$-20.94^{+0.43}_{-0.21}$ [31]	0.139	–20.5	–20.199
	1.790(40) [32]	$-20.10^{+0.18}_{-0.13}$ [32]	0.333	–20.466	–20.172
	1.800(400) [58]	$-20.12^{+0.78}_{-0.26}$ [58]	0.35	–20.469	–20.175
^{16}Ne	1.400(20) [40]	$-20.38^{+0.20}_{-0.13}$ [40]	1.312	–18.767	–17.961
^{19}Mg	0.750(50) [37]	$-11.40^{+0.14}_{-0.20}$ [37]	–2.473	–13.572	–12.885
^{45}Fe	1.100(100) [33]	$-2.40^{+0.26}_{-0.26}$ [33]	–1.818	–3.917	–2.35
	1.14(50) [34]	$-2.07^{+0.24}_{-0.21}$ [34]	–2.635	–4.404	–2.838
	1.154(16) [36]	$-2.55^{+0.13}_{-0.12}$ [36]	–2.318	–4.567	–3.001
	1.210(50) [59]	$-2.42^{+0.03}_{-0.03}$ [59]	–3.076	–5.195	–3.629
^{48}Ni	1.290(40) [60]	$-2.52^{+0.24}_{-0.22}$ [60]	–2.134	–4.353	–2.712
	1.350(20) [36]	$-2.08^{+0.40}_{-0.78}$ [36]	–3.191	–4.97	–3.328
	1.310(40) [54]	$-2.52^{+0.24}_{-0.22}$ [54]	–2.344	–4.563	–2.922
^{54}Zn	1.280(210) [55]	$-2.76^{+0.15}_{-0.14}$ [55]	–2.174	–4.633	–1.149
	1.480(20)[35]	$-2.43^{+0.20}_{-0.14}$ [35]	–2.578	–4.707	–2.925
^{67}Kr	1.690(17) [38]	$-1.70^{+0.02}_{-0.02}$ [38]	–0.877	–2.276	–0.286

To assess the accuracy of the predicted half-life, we calculate the standard deviation between the experimental and computed half-lives using the following equation:

$$\sigma = \left\{ \frac{1}{n} \sum_{i=1}^{n} \left(log_{10} T_i - log_{10} T_{Exp} \right)^2 \right\}^{1/2} . \qquad (14)$$

We found that the predicted half-life shows a higher standard deviation of σ = 1.73 compared to the previous models. In the second part of the study, we investigated the relationship between the experimental formation probability of two-proton radioactivity and the cube root of the atomic mass number of the daughter nucleus ($A_d^{1/3}$) in order to reduce the standard deviation. We utilized the theoretically predicted half-lives in higher angular momentum states due to a lack of experimental data in these states. In Fig. 2, we plotted the experimental formation probability against $A_d^{1/3}$ for angular momentum states l = 0, 2, and 4. We found a linear relationship between the logarithm of the formation probability and $A_d^{1/3}$ for these angular momentum states using linear fitting, expressed as:

$$\log_{10} S_{2p} = a_l A_d^{1/3} + b_l , \qquad (15)$$

where the parameters a_l and b_l correspond to each specific angular momentum state. For l = 0, the parameters are a_0 = –0.943394 and b_0 = 1.43779. For l = 2, the parameters are a_2 = –3.52698 and b_2 = 9.90015. For l = 4, the parameters are a_4 = –0.326634 and b_4 = –1.33126.

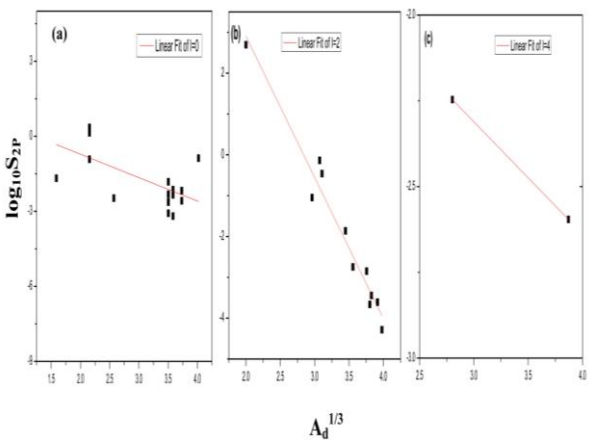

Fig. 2. Variation of the logarithmic formation probability with the cube root of the atomic mass number of the daughter nuclei for angular momentum states: *a* – l = 0; *b* – l = 2; *c* – l = 4.

We calculated the half-life for experimentally observed decay cases using the proposed formula for the formation probability, which is given in the sixth column of Table 1. The proposed formula significantly improved the accuracy of half-life predictions

by reducing the standard deviation from 1.73 to 1.09. We compared the calculated half-lives with the predictions of other theoretical models, such as the ELDM [28], the GLDM [27], the SEB [6], the GLM [7], and the UFM [12], as well as empirical formula predictions [29, 30] in Table 2. Table 2 shows that the calculated half-lives are in very good agreement with the experimental values and other theoretical predictions. The standard deviation of the decay half-life calculated for other models is given in Table 3. The predicted half-life shows the lowest standard deviation value of 1.09 compared to the ELDM [28], the GLDM [27], the SEB [6], the GLM [7], and the UFM [12], as well as the empirical formula predictions [29, 30]. We also compared our results with other theoretical predictions graphically by plotting a graph between the hindrance factor $\log_{10}\left(T_{1/2}^{Cal}/T_{1/2}^{Exp}\right)$ and the number of parent nuclei in Fig. 3. The predicted half-life exhibits a logarithmic difference in the range of –1.62 to 2.42. This range of deviation is the smallest compared to other theoretical predictions. The ELDM model (–0.46 to 3.78), the GLDM model (–1.16 to 3.75), the SEB model (–0.92 to 4.67), the GLM model (–1.13 to 3.95), and the UFM model (–0.83 to 3.7) show a higher range of deviation compared to our predictions. The empirical formula proposed by Sreeja et al. (–2.44 to 4.22) and the formula proposed by Liu et al. (–4.3 to 2.61) exhibit a wider range of deviations. The logarithmic difference value is less than one in most decay cases, demonstrating the accuracy of our predictions. The ^{16}Ne nucleus shows a higher deviation of 2.42, but this value is the lowest compared to earlier theoretical predictions. The Figure illustrates that the predicted half-life using the proposed linear formation probability formula is better suited for reproducing experimental data.

Table 2. **The computed logarithmic half-live of two-proton decays for various isotopes compared with other model predictions, formula predictions, and experimental values**

Nucleus	Q_{2p}^{Exp}, MeV	$\log_{10}T_{1/2}$, s							
		Experiment	Present	$EF_{(s)}$ [29]	GLDM [27]	GNL [30]	GLM [7]	SEB [6]	UFM [11]
^{6}Be	1.371(5) [38]	–19.51 [38]	–21.127	–21.952	–19.37	–23.81	–19.70	–19.86	–19.41
^{12}O	1.638(24) [57]	–19.4 [57]	–19.724	–18.467	–19.17	–20.17	–18.04	–17.70	–18.45
	1.820(120) [31]	$-20.94^{+0.43}_{-0.21}$ [31]	–20.199	–18.79	–19.46	–20.52	–18.30	–18.03	–18.69
	1.790(40) [32]	$-20.10^{+0.18}_{-0.13}$ [32]	–20.172	–18.74	–19.43	–20.46	–18.26	–17.98	–18.65
	1.800(400) [58]	$-20.12^{+0.78}_{-0.26}$ [58]	–20.175	–18.76	–19.44	–20.48	–18.27	–18.00	–18.66
^{16}Ne	1.400(20) [40]	$-20.38^{+0.20}_{-0.13}$ [40]	–17.961	–16.16	–16.63	–17.77	–16.43	–15.71	–16.68
^{19}Mg	0.750(50) [37]	$-11.40^{+0.14}_{-0.20}$ [37]	–12.885	–10.66	–11.79	–12.03	–11.46	–10.58	–11.77
^{45}Fe	1.100(100) [33]	$-2.40^{+0.26}_{-0.26}$ [33]	–2.35	–1.81	–2.23	–2.21	–2.09	–2.32	–1.94
	1.14(50) [34]	$-2.07^{+0.24}_{-0.21}$ [34]	–2.838	–1.76	–2.71	–2.64	–2.58	–2.67	–2.43
	1.154(16) [36]	$-2.55^{+0.13}_{-0.12}$ [36]	–3.001	–1.81	–2.87	–2.79	–2.74	–2.78	–2.60
	1.210(50) [59]	$-2.42^{+0.03}_{-0.03}$ [59]	–3.629	–1.66	–3.50	–3.35	–3.37	–3.24	–3.23
^{48}Ni	1.290(40) [60]	$-2.52^{+0.24}_{-0.22}$ [60]	–2.712	–1.61	–2.62	–2.59	–2.59	–2.55	–2.29
	1.350(20) [36]	$-2.08^{+0.40}_{-0.78}$ [36]	–3.328	–2.13	–3.24	–3.13	–3.21	–3.00	–2.91
	1.310(40) [54]	$-2.52^{+0.24}_{-0.22}$ [54]	–2.922		–2.83				–2.50
^{54}Zn	1.280(210) [55]	$-2.76^{+0.15}_{-0.14}$ [55]	–1.149	–0.10	–0.87	–1.01	–0.93	–1.31	–0.52
	1.480(20)[35]	$-2.43^{+0.20}_{-0.14}$ [35]	–2.925	–1.83	–2.95	–2.81	–3.01	–2.81	–2.61
^{67}Kr	1.690(17) [38]	$-1.70^{+0.02}_{-0.02}$ [38]	–0.286	0.31	–1.25	–0.58	–0.76	–0.95	–0.54

Table 3. **The standard deviation σ between the experimental data and the predicted half-life values using different theoretical models and formulas**

Model	Present $S_{2p} = 0.5$	Present S_{2p}	$EF_{(s)}$ [29]	GLDM [27]	GNL [30]	GLM [7]	SEB [6]	UFM [12]	ELDM [28]
σ	1.73	1.09	1.72	1.2	1.45	1.55	1.73	1.38	1.53
Cases	17	17	16	17	16	16	16	17	8

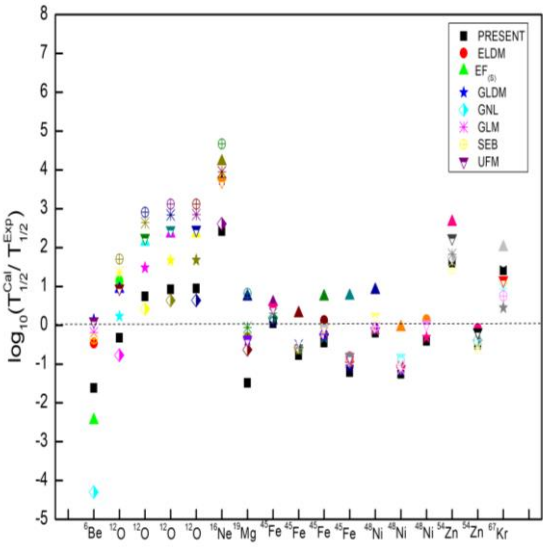

Fig. 3. Comparison of the hindrance factor $\log_{10}\left(T_{1/2}^{Cal}/T_{1/2}^{Exp}\right)$ and the number of parent nuclei using different models and empirical formulas. (See color Figure on the journal website.)

We extended the half-life predictions to other energetically possible decay cases and compared them with different theoretical half-lives. Using the proposed formula, we calculated the formation probability and tabulated it in the fourth column of Table 4. Utilizing the formation probability, we computed the corresponding half-lives of ground states and listed them in the fifth column of Table 4. The computed logarithmic half-life of two-proton decays for various isotopes in the ground state (l = 0) is provided in Table 4. We compared our results with the predictions of the ELDM [28], the GLDM [27], the SEB [6], the GLM [7], and the UFM [12], as well as the empirical formula predictions [29, 30] in Table 4. We found that the computed half-lives agree with the previous theoretical predictions. For the comparative study, we plotted graphs between the previously predicted logarithmic half-lives and the atomic number of the emitter nucleus in Figs. 4 and 5. These Figures clearly illustrate that the predicted half-life is in good agreement with previous theoretical predictions.

Table 4. **The computed logarithmic half-live of two proton decays in ground states (l = 0) for various isotopes is compared with other theoretical predictions**

Nucleus	Q_{2p}^{Exp}, MeV	l value	S_{2p}	$\log_{10}T_{1/2}$, s						
				Present	$EF_{(s)}$ [29]	GLDM [27]	GNL [30]	GLM [7]	SEB [6]	UFM [12]
^{7}B	1.420	0	0.668	–21.364	–20.911		–22.725			–19.33
^{13}F	3.09	0	0.219	–20.711	–19.592		–21.349			–19.33
^{15}Ne	2.528	0	0.166	–20.008	–18.382		–20.087			–18.57
^{16}Ne	1.401	0	0.146	–18.204	–16.163		–17.771			
^{17}Na	4.027	0	0.129	–20.505	–19.219		–20.959			–18.95
^{22}Si	1.283	0	0.075	–14.771	–12.296	–13.295	–13.735	–13.25	–12.17	–14.61
^{26}S	1.755	0	0.052	–15.172	–12.707	–14.593	–14.165	–13.92	–12.82	–16.09
^{29}Ar	5.90	0	0.041	–19.739	–17.479		–19.144			–18.99
^{30}Ar	2.280	0	0.037	–15.508	–12.995		–14.465			–17.02
^{33}Ca	5.13	0	0.03	–18.732	–16.165		–17.773			–18.11
^{34}Ca	1.474	0	0.028	–11.011	–8.65	–10.7	–9.932	–10.10	–8.99	–14.46
^{36}Sc	1.993	0	0.024	–12.774	–10.302		–11.655	–12.00	–10.79	
^{37}Ti	5.40	0	0.022	–18.358	–15.641		–17.226			–17.81
^{38}Ti	2.743	0	0.021	–14.54	–11.93	–14.271	–13.354	–13.84	–12.70	–15.18
^{39}V	4.21	0	0.02	–16.778	–14.005		–15.52			–16.34
^{40}V	1.842	0	0.018	–10.798	–8.457		–9.73	–10.15	–8.97	–11.66
^{41}Cr	3.33	0	0.017	–14.908	–12.195		–13.63			–14.53
^{42}Cr	1.002	0	0.016	–3.336	–1.782	–2.876	–2.765	–2.65	–2.87	–7.4
^{44}Mn	0.50	0	0.014	8.969	8.987		8.472			9.8
^{47}Co	1.042	0	0.012	–0.889	0.207		–0.69	–0.42	–1.13	
^{48}Ni	1.309	0	0.011	–3.144	–1.781		–2.764			
^{49}Ni	0.492	0	0.011	13.863	12.776	14.462	12.425	14.54		0.23
^{56}Ga	2.443	0	0.007	–8.577	–6.422		–7.606	–8.57	–7.41	–10.3
^{58}Ge	3.732	0	0.007	–12.267	–9.53	–2.3098	–10.849	–12.32	–11.10	–11.19
^{59}Ge	2.102	0	0.006	–6.221	–4.437	–6.975	–5.536	–6.31	–5.41	–2.73
^{60}Ge	0.631	0	0.006	14.074	12.404	13.547	12.037	14.24		
^{61}As	2.282	0	0.006	–6.597	–4.738		–5.85	–6.76	–5.78	–4.95
^{63}Se	2.36	0	0.005	–6.389	–4.565		–5.668			–6.59
^{64}Se	0.70	0	0.005	14.327	12.394		12.027			14.39

Continuation of Table 4

Nucleus	Q_{2p}^{Exp}, MeV	l value	S_{2p}	$\log_{10}T_{1/2}$, s						
				Present	$EF_{(s)}$ [29]	GLDM [27]	GNL [30]	GLM [7]	SEB [6]	UFM [12]
^{66}Br	1.39	0	0.005	2.15	2.24		1.432			1.83
^{68}Kr	1.46	0	0.004	1.958	2.221		–0.58			1.83
^{81}Mo	0.73	0	0.002	23.325	18.749		1.412			23.26
^{85}Ru	1.13	0	0.002	14.279	11.588		18.657			14.08
^{108}Xe	1.01	0	0.001	27.449	20.872		11.186			27.07

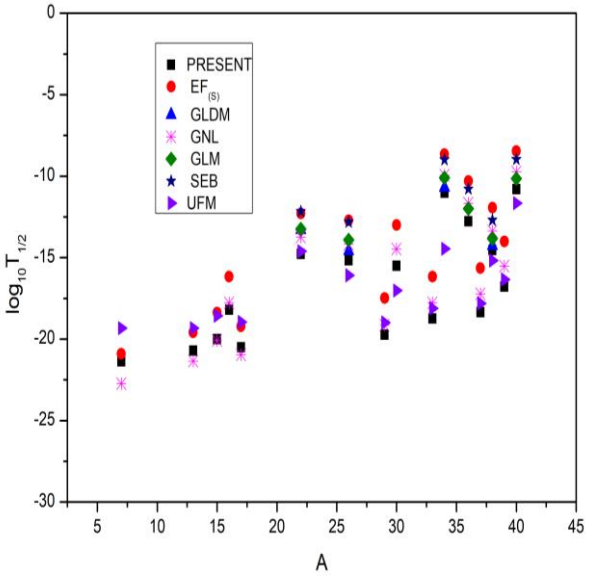

Fig. 4. Comparison of computed logarithmic half-lives of two-proton decays for various isotopes with previous theoretical predictions. (See color Figure on the journal website.)

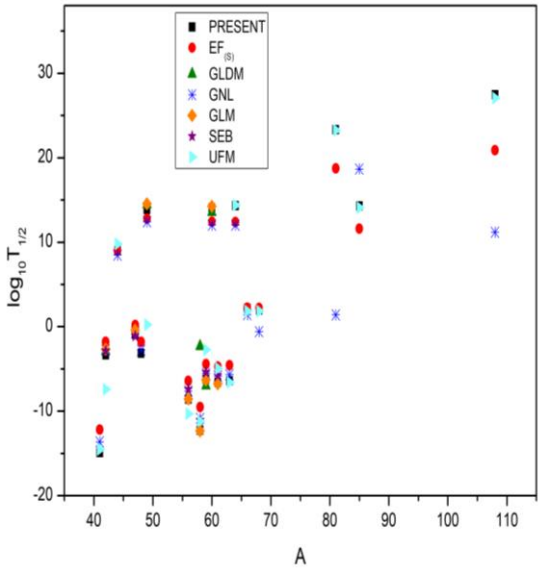

Fig. 5. Comparison of computed logarithmic half-lives of two-proton decays for various isotopes with previous theoretical predictions. (See color Figure on the journal website.)

We performed a least squares fit analysis to generalize this linear formula for different angular momentum states. We obtained a polynomial relationship between the angular momentum l value and the slope of the linear formula.

$$m_l = (c \cdot l^2) + (d \cdot l) + e, \qquad (16)$$

where the parameters c = 0.72299, d = –2.73778, and e = –0.94339. Similarly, we also obtained another polynomial relation between the angular momentum l value and the intercept.

$$C_l = \left(c \cdot l^2\right) + \left(d \cdot l\right) + e, \qquad (17)$$

where the parameters c = –2.46172, d = 9.15462, and e = 1.43779. Using the relation slope and intercept with l value, we can generalize the formula as

$$log_{10}S_{2p} = m_l A_d^{1/3} + c_l. \qquad (18)$$

Using this generalized formula, we were able to compute the formation probability of two-proton radioactivity for all angular momentum states. We calculated the half-life of two-proton decay for angular states l = 1 and l = 3 in Table 5 using the generalized expression.

Table 5. **The computed logarithmic half-live of two proton decays in higher angular momentum states for various isotopes is compared with other theoretical predictions**

Nucleus	Q_{2p}^{Exp}, MeV	l value	$\log_{10}T_{1/2}$, s							
			Present	ELDM [28]	$EF_{(s)}$ [29]	GLDM [27]	GNL [30]	GLM [7]	SEB [6]	UFM [12]
^{10}N	1.30	1	–22.158	–17.644	–20.035	–18.59	–18.591	–17.36	–16.76	–18.07
^{28}Cl	1.965	2	–14.897	–12.947	–14.517		–12.457	–13.11	–11.78	–15.29
^{31}K	5.66	2	–19.132		–19.43		–17.577			–18.21
^{32}K	2.077	2	–13.701	–12.248	–13.459		–11.554	–12.49	–11.32	–14.44

Continuation of Table 5

Nucleus	Q_{2p}^{Exp}, MeV	l value	$\log_{10}T_{1/2}$, s							
			Present	ELDM [28]	$EF_{(s)}$ [29]	GLDM [27]	GNL [30]	GLM [7]	SEB [6]	UFM [12]
^{43}Mn	2.48	2	–10.82		–10.952		–9.446			–10.65
^{47}Co	1.02	2	1.070		0.82		1.983			1.13
^{55}Zn	0.78	2	9.283		8.238		8.987			8.77
^{57}Ga	2.047	2	–4.393	–5.300	–5.215		–4.14	–5.91	–4.94	–3.01
^{58}Ga	0.51	2	19.89		18.256		18.63			18.71
^{62}As	0.692	2	15.781	14.519	13.829		14.176	14.06		17.99
^{65}Br	2.43	2	–3.6		–4.8		–3.906			–5.55
^{35}Sc	4.98	3	–16.86		–19.048		–16.033			–16.1
^{24}P	1.24	4	–8.5		–14.342		–10.049			–8.5
^{60}As	3.492	4	–8.37	–8.682	–10.84		–8.332	–9.40	–7.88	–8.37

The half-life values obtained from our calculations were then compared with the predictions from five different theoretical models and two empirical formulas. These predicted half-lives show good agreement with previous theoretical predictions.

4. Conclusion

In summary, we systematically studied the two-proton radioactivity of nuclei with Z < 54 using the TPA with a cosh-type potential. The model predicts the half-life with the lowest standard deviation compared to the experimental half-lives when using V_0 = 58.405 MeV and a = 0.537 fm as parameters for depth and diffuseness. By examining the formation probability, we found a linear relationship between the formation probability of two-proton radioactivity and the cube root of the atomic mass number of the daughter nuclei, which is similar to the formula Chen et al. [45] proposed in the case of one-proton decay. The linear formula for formation probability predicts the half-life with the lowest standard deviation (σ = 1.09) compared to previous models and empirical formulas. This lowest standard deviation indicates that the proposed formula is suitable for studying two-proton decay. Using the curve-fitting method, we generalised the linear formula for the formation probability to all angular momentum states.

REFERENCES

1. Y.B. Zeldovich. The existence of new isotopes of light nuclei and the equation of state of neutrons. Sov. Phys. JETP 38 (1960) 1123.
2. V.I. Goldanskii. The influence of pairing in the passage of two particles through the potential barrier. Phys. Lett. 14 (1965) 233.
3. V.I. Goldansky. Two-proton radioactivity. Nucl. Phys. 27 (1961) 648.
4. J. Jänecke. The emission of protons from light neutron-deficient nuclei. Nucl. Phys. 61 (1965) 326.
5. V.M. Galitsky, V.F. Cheltsov. Two-proton radioactivity theory. Nucl. Phys. 56 (1964) 86.
6. Y.-T. Zou et al. Systematic study of two-proton radioactivity with a screened electrostatic barrier. Chinese Phys. C 45 (2021) 104101.
7. H.-M. Liu et al. Systematic study of two-proton radioactivity within a Gamow-like model. Chinese Phys. C 45 (2021) 044110.
8. F.C. Barker. ^{12}O ground-state decay by ^{2}He emission. Phys. Rev. C 63 (2001) 047303.
9. L.V. Grigorenko, M.V. Zhukov. Two-proton radioactivity and three-body decay. III. Integral formulas for decay widths in a simplified semianalytical approach. Phys. Rev. C 76 (2007) 014008.
10. R. Álvarez-Rodríguez et al. Distinction between sequential and direct three-body decays. Phys. Rev. Lett. 100 (2008) 192501.
11. D.-X. Zhu et al. Two-proton radioactivity within Coulomb and proximity potential model. Chinese Phys. C 46 (2022) 044106.
12. F. Xing et al. Two-proton radioactivity of ground and excited states within a unified fission model. Chinese Phys. C 45 (2021) 124105.
13. M.G. Srinivas et al. Exploring new proton emitting isotopes of Lanthanides. Indian J. Phys. 97 (2023) 203.
14. M.G. Srinivas et al. A Systematic Study of Proton Decay in Superheavy Elements. Ukr. J. Phys. 67 (2022) 631.
15. M.G. Srinivas et al. Systematics of proton decay of actinides. Indian J. of Pure Ap. Phys. 58 (2020) 255.
16. M.G. Srinivas et al. Proton decay of actinide nuclei. Nucl. Phys. A 995 (2020) 121689.
17. M.G. Srinivas et al. A systematic analysis for one proton radioactivity of ground state nuclei. Nucl. Phys. A 1036 (2023) 122673.
18. M.G. Srinivas et al. Semi-empirical formulae for one- and two-proton radioactivity. Indian J. Phys. 97 (2023) 1181.
19. H.C. Manjunatha et al. proton radioactivity of heavy nuclei of atomic number range 72 < Z< 88. Phys. Part.

Nuclei Lett. 17 (2020) 909.
20. H.C. Manjunatha et al. Investigations on the superheavy nuclei with magic number of neutrons and protons. Int. J. Mod. Phys. E 29(05) (2020) 2050028.
21. N.P. Saeed Abdulla, M.K. Preethi Rajan, R.K. Biju. Systematic study of two proton radioactivity within the effective liquid drop model. Phys. Scripta 99(3) (2024) 035310.
22. N.S. Abdulla, M.P. Preethi Rajan, R.K. Biju. An empirical formula for the two-proton decay half-lives in the ground and excited states. Nucl. Part. Phys. Proc. 339-340 (2023) 43.
23. N.P. Saeed Abdulla, M.K. Preethi Rajan, R.K. Biju. An empirical formula for the half-lives of one- and two-proton radioactivity. Int. J. Mod. Phys. E 33 (2024) 2450007.
24. X. Pan et al. Systematic study of two-proton radioactivity half-lives using the two-potential and Skyrme-Hartree-Fock approaches. Chinese Phys. C 45 (2021) 124104.
25. B.A. Brown, F.C. Barker. Di-proton decay of ^{45}Fe. Phys. Rev. C 67 (2003) 041304(R).
26. J. Rotureau, J. Okołowicz, M. Płoszajczak. Theory of the two-proton radioactivity in the continuum shell model. Nucl. Phys. A 767 (2006) 13.
27. J.P. Cui et al. Two-proton radioactivity within a generalized liquid drop model. Phys. Rev. C 101 (2020) 014301.
28. M. Gonçalves et al. Two-proton emission half-lives in the effective liquid drop model. Phys. Lett. B 774 (2017) 14.
29. I. Sreeja, M. Balasubramaniam. An empirical formula for the half-lives of exotic two-proton emission. Eur. Phys. J. A 55 (2019) 33.
30. H.-M. Liu et al. New Geiger-Nuttall law for two-proton radioactivity. Chinese Phys. C 45 (2021) 024108.
31. G.J. KeKelis et al. Masses of the unbound nuclei ^{16}Ne, ^{15}F, and ^{12}O. Phys. Rev. C 17 (1978) 1929.
32. R.A. Kryger et al. Two-proton emission from the ground state of ^{12}O. Phys. Rev. Lett. 74 (1995) 860.
33. M. Pfützner et al. First evidence for the two-proton decay of ^{45}Fe. Eur. Phys. J. A 14 (2002) 279.
34. J. Giovinazzo et al. Two-proton radioactivity of ^{45}Fe. Phys. Rev. Lett. 89 (2002) 102501.
35. B. Blank et al. First observation of ^{54}Zn and its decay by two-proton emission. Phys. Rev. Lett. 94 (2005) 232501.
36. C. Dossat et al. Two-proton radioactivity studies with ^{45}Fe and ^{48}Ni. Phys. Rev. C 72 (2005) 054315.
37. I. Mukha et al. Observation of two-proton radioactivity of ^{19}Mg by tracking the decay products. Phys. Rev. Lett. 99 (2007) 182501.
38. T. Goigoux et al. Two-proton radioactivity of ^{67}Kr. Phys. Rev. Lett. 117 (2016) 162501.
39. W. Whaling. Magnetic analysis of the Li^6 (He^3, t) Be^6 reaction. Phys. Rev. 150 (1966) 836.
40. C.J. Woodward, R.E. Tribble, D.M. Tanner. Mass of ^{16}Ne. Phys. Rev. C 27(1983) 27.
41. B. Buck, A.C. Merchant, S.M. Perez. α decay calculations with a realistic potential. Phys. Rev. C 45 (1992) 2247.
42. B. Buck, A.C. Merchant, S.M. Perez. Alpha-cluster structure in ^{212}Po. Phys. Rev. Lett. 72 (1994) 1326.
43. J.-G. Deng et al. α decay properties of ^{296}Og within the two-potential approach. Chinese Phys. C 42 (2018) 044102.
44. X.-D. Sun et al. Systematic study of α decay half-lives of doubly odd nuclei within the two-potential approach. Phys. Rev. C 95 (2017) 044303.
45. J.-L. Chen et al. Systematic study on proton radioactivity of spherical proton emitters within two-potential approach. Eur. Phys. J. A 57 (2021) 305.
46. H.-F. Zhang et al. Theoretical analysis and new formulae for half-lives of proton emission. Chinese Phys. Lett. 26 (2009) 072301.
47. Y. Lim, X. Xia, Y. Kim. Proton radioactivity in relativistic continuum Hartree-Bogoliubov theory. Phys. Rev. C 93 (2016) 014314.
48. A. Soylu et al. Proton radioactivity half-lives with nuclear asymmetry factor. Chinese Phys. C 45 (2021) 044108.
49. Q. Zhao et al. Proton radioactivity described by covariant density functional theory with the similarity renormalization group method. Phys. Rev. C 90 (2014) 054326.
50. B. Nerlo-Pomorska, K. Pomorski. Simple formula for nuclear charge radius. Zeitschrift für Physik. A 348 (1994) 169.
51. J.J. Morehead. Asymptotics of radial wave equations. J. Math. Phys. 36 (1995) 5431.
52. B. Buck, A. C. Merchant, S. M. Perez. Ground state proton emission from heavy nuclei. Phys. Rev. C 45 (1992) 1688.
53. N.G. Kelkar, H.M. Castañeda. Critical view of WKB decay widths. Phys. Rev. C 76 (2007) 064605.
54. M. Wang et al. The AME2016 atomic mass evaluation. (II). Tables, graphs and references. Chinese Phys. C 41(2017) 030003.
55. P. Ascher et al. Direct observation of two protons in the decay of ^{54}Zn. Phys. Rev. Lett. 107 (2011) 102502.
56. D.S. Delion, R.J. Liotta, R. Wyss. Theories of proton emission. Phys. Rep. 424 (2006) 113.
57. M.F. Jager et al. Two-proton decay of ^{12}O and its isobaric analog state in ^{12}N. Phys. Rev. C 86 (2012) 011304.
58. D. Suzuki et al. Breakdown of the Z = 8 shell closure in unbound ^{12}O and its mirror symmetry. Phys. Rev. Lett. 103 (2009) 152503.
59. L. Audirac et al. Direct and β-delayed multi-proton emission from atomic nuclei with a time projection chamber: the cases of ^{43}Cr, ^{45}Fe, and ^{51}Ni. Eur. Phys. J. A 48 (2012) 179.
60. M. Pomorski et al. Proton spectroscopy of ^{48}Ni, ^{46}Fe, and ^{44}Cr. Phys. Rev. C 90 (2014) 014311.

Н. П. Саїд Абдулла[1], А. Павітран[1], М. К. Преті Раджан[2], Р. К. Біджу[1,3,*]

[1] Факультет фізики, Державний коледж Бреннен, Дхармадам, Талассері, штат Керала, Індія
[2] Факультет фізики, Коледж Пайянур, Університет Каннур, Пайянур, Каннур, штат Керала, Індія
[3] Факультет фізики, Коледж Пажассі Раджа Н. С. С., Маттанур, Університет Каннур, Каннур, штат Керала, Індія

*Відповідальний автор: bijurkn@gmail.com

ДОСЛІДЖЕННЯ ДВОПРОТОННОГО РОЗПАДУ З ВИКОРИСТАННЯМ МОДИФІКОВАНОЇ ІМОВІРНОСТІ ФОРМУВАННЯ

Досліджено двопротонну радіоактивність за допомогою двопотенціального підходу з потенціалом типу cosh для розрахунків періодів напіврозпаду. Параметри глибини $V_0 = 58{,}405$ МеВ і дифузності $a = 0{,}537$ Фм в ядерному cosh-потенціалі показали найменше стандартне відхилення між розрахунковими і експериментальними періодами напіврозпаду. Ми запропонували формулу для ймовірності формування з використанням лінійної залежності між $\log_{10} S_{2p}$ та $A_d^{1/3}$ для кутового моменту $l = 0$, 2 і 4. Модель досягла найменшого стандартного відхилення ($\sigma = 1{,}09$) за допомогою цієї лінійної формули порівняно з попередніми моделями та емпіричними формулами. Запропонована формула значно підвищила точність розрахунків періоду напіврозпаду через зменшення стандартного відхилення з 1,73 до 1,09. Розрахунки дають для фактора подавлення діапазон значень від −1,62 до 2,42, що є найнижчим порівняно з попередніми теоретичними прогнозами. Лінійна формула для ймовірності формування була узагальнена для різних станів кутового моменту за допомогою методу найменших квадратів. Розширено розрахунки періоду напіврозпаду та ймовірності утворення для 48 ядер, і одержані значення добре узгоджуються з результатами, отриманими з попередніми п’ятьма теоретичними моделями і двома емпіричними формулами.

Ключові слова: двопотенціальний підхід, ймовірність формування.

Надійшла / Received 08.11.2023